재 료 상 변 태

Phase Transformation of Materials

2008. 10. 28.

박 은 수

서울대학교 재료공학

Contents for previous class

- **Boundaries in Single-Phase Solids**

  (a) Low-Angle and High-Angle Boundaries

  (b) Special High-Angle Grain Boundaries

  (c) Equilibrium in Polycrystalline Materials

Contents for today's class

- **Thermally Activated Migration of Grain Boundaries**
- **The Kinetics of Grain Growth**
- **Interphase Interfaces in Solid**

3.3.4. Thermally Activated Migration of Grain Boundaries

If the boundary is curved in the shape of cylinder, Fig. 3.20a, it is acted on by a force of magnitude γ/r towards its center of curvature.

Therefore, the only way the boundary tension forces can balance in three dimensions is if the boundary is planar ($r = \infty$) or if it is curved with equal radii in opposite directions, Fig. 3.20b and c.

Net Force due to Surface Tension

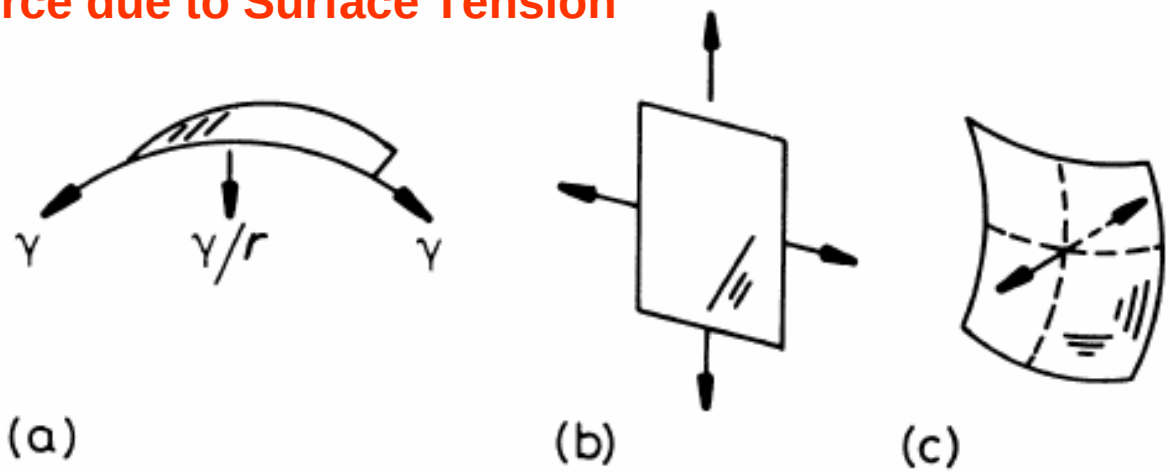

Equilibrium angle at each boundary junction in 3D? →109°28'

Fig. 3.20 (a) A cylindrical boundary with a radius of curvature r is acted on by a force γ/r. (b) A planar boundary with no net force. (c) A doubly curved boundary with no net force.

Direction of Grain Boundary Migration during Grain Growth

For isotropic grain boundary energy in two dimensions,

Equilibrium angle at each boundary junction? →120°

Morphology of metastable equilibrium state

Boundaries around Grain < 6

- grain shrink, disappear

Boundaries around Grain = 6

; equilibrium

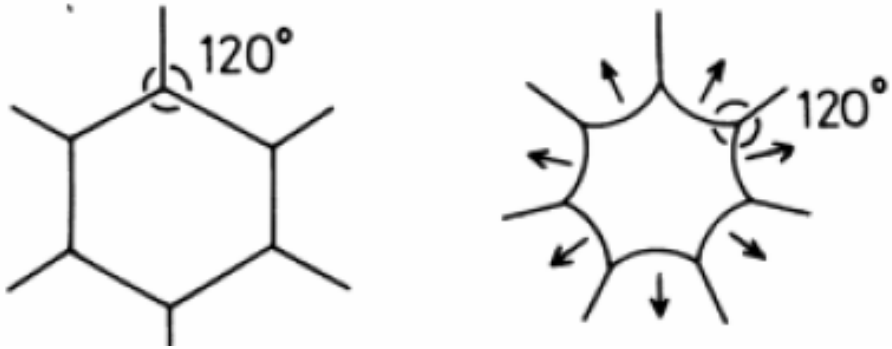

Boundaries around Grain > 6 - grain growth

Reduce the # of grains, increase the mean grain size, reducing the total G.B. energy

Called grain growth (or grain coarsening): at high temperature above about 0.5 T_m

Grain Growth (Soap Bubble Model)

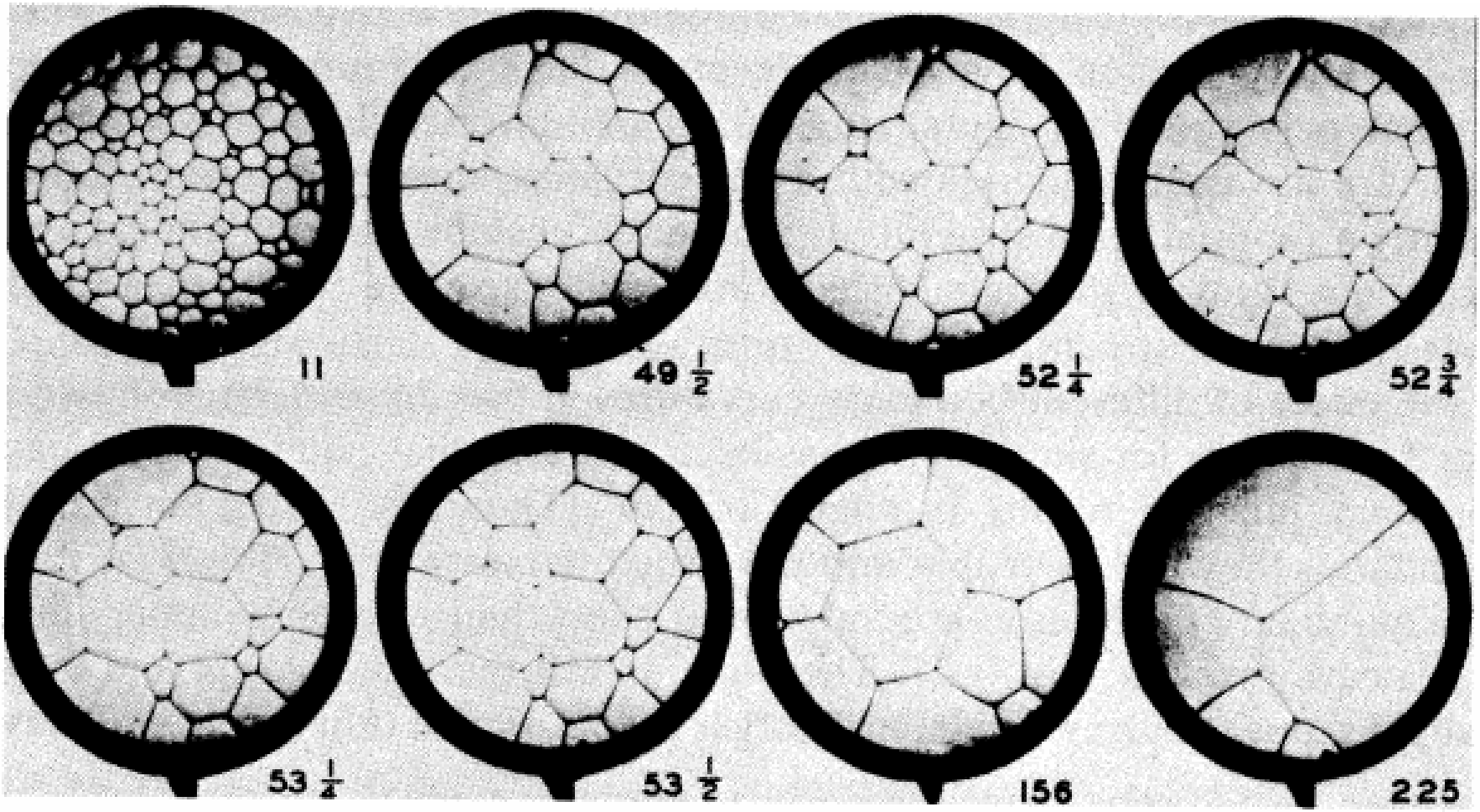

Fig. 3.22 Two-dimensional cells of a soap solution illustration the process of grain growth. Numbers are time in minutes. (After C.S. Smith, Metal Interfaces, American Society for Metals, 1952, p. 81.)

Example of Grain Growth simulation in 3D

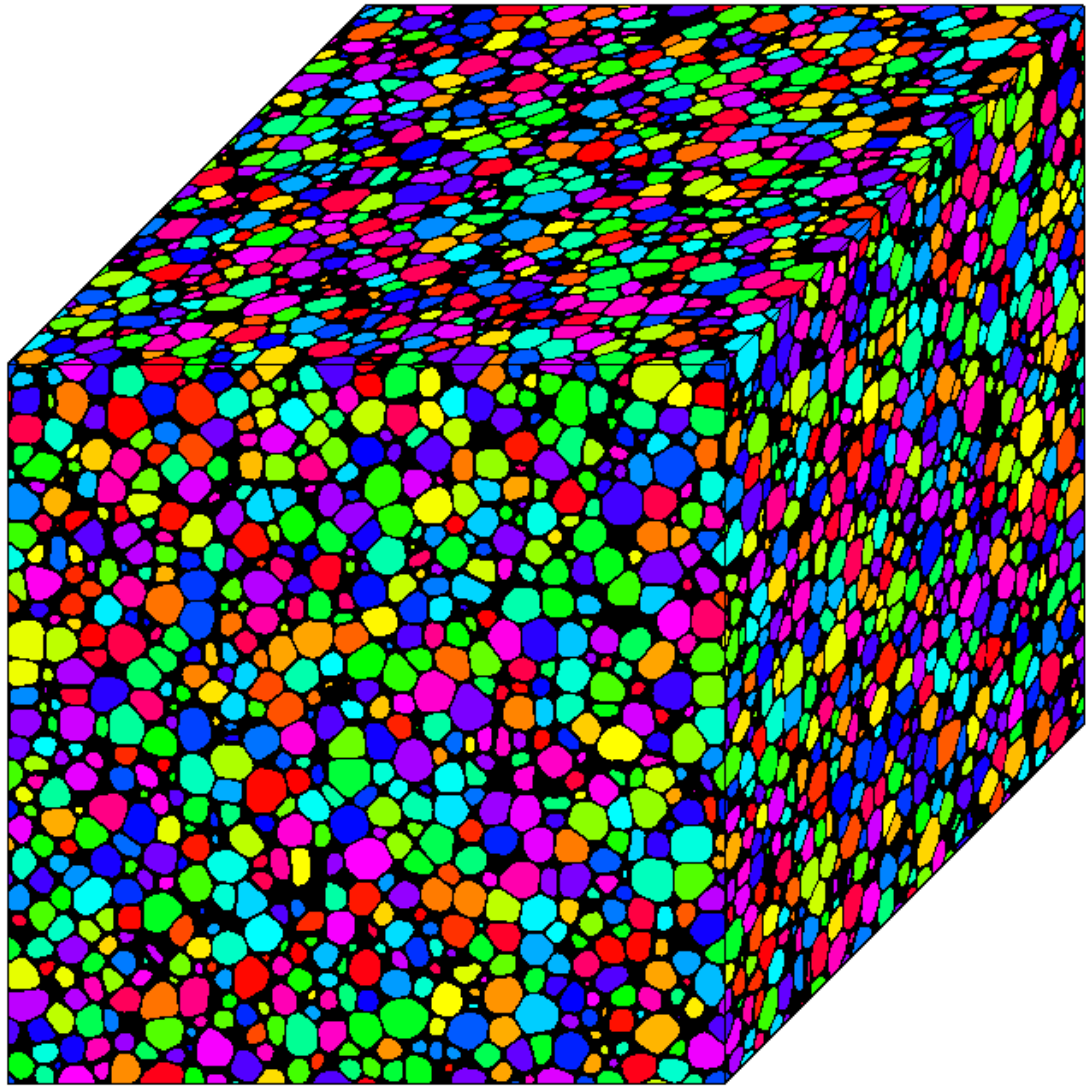

Example of Grain Growth simulation in 3D

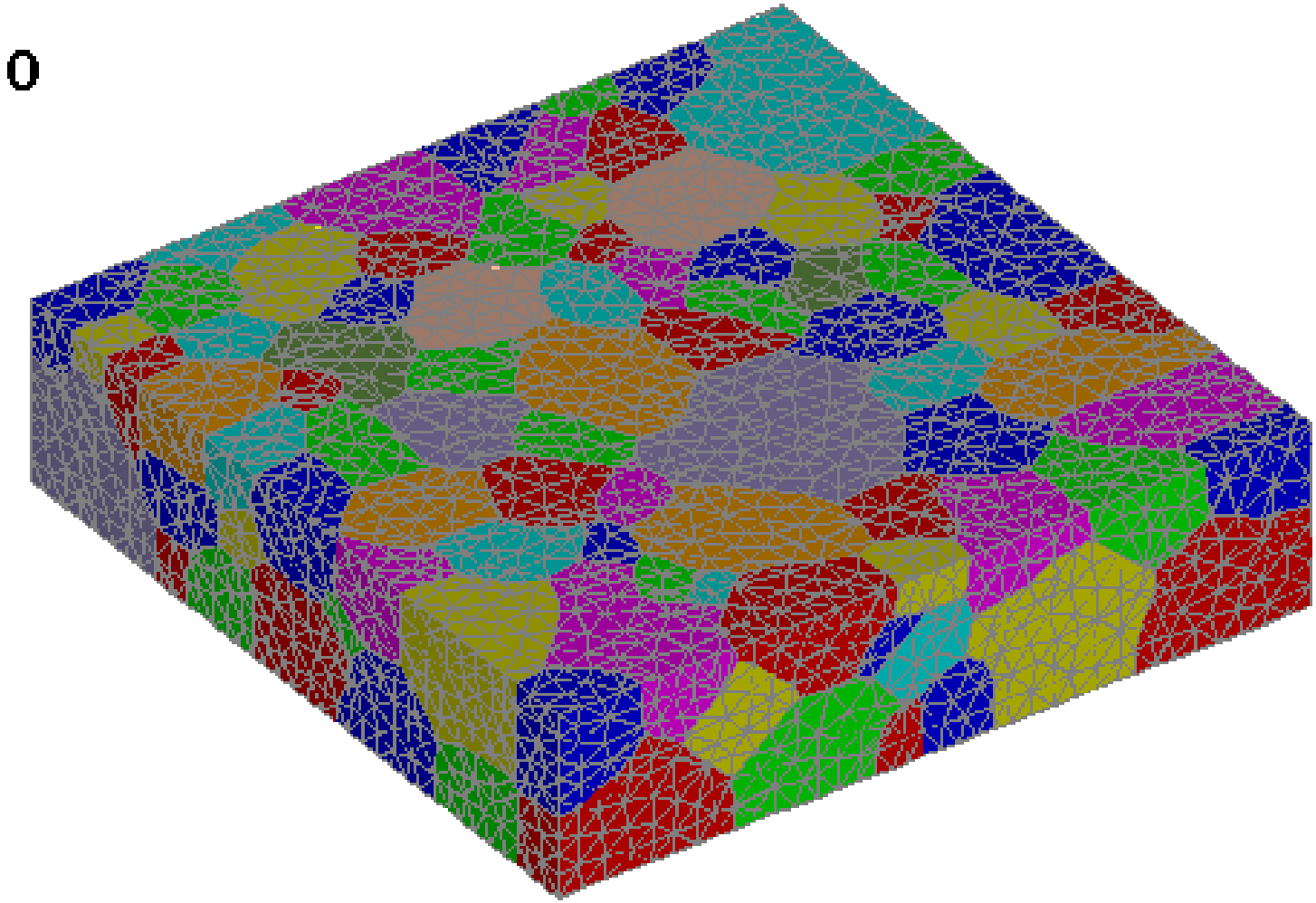

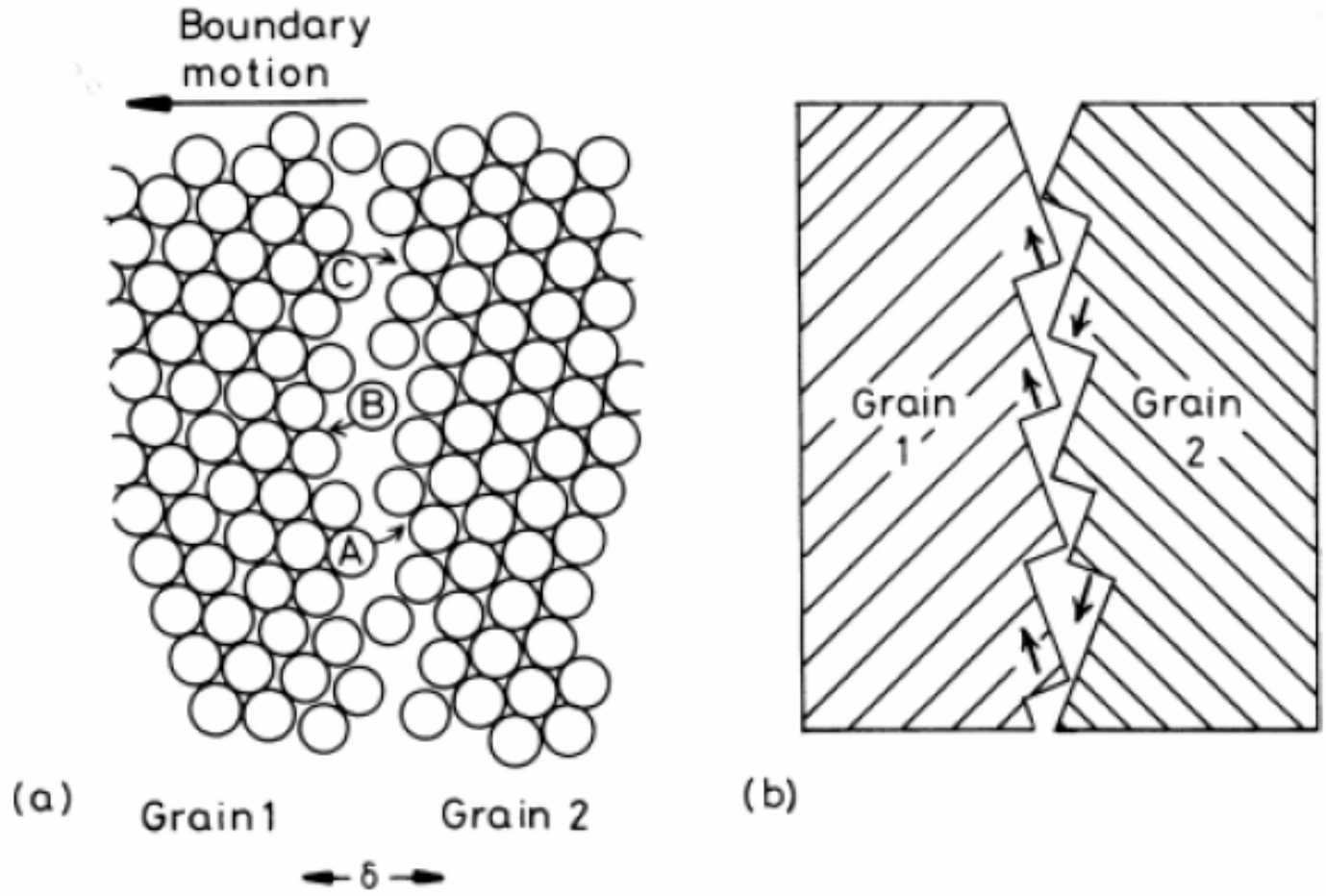

Fig. 3.23 (a) The atomic mechanism of boundary migration. The boundary migrates to the left if the jump rate from grain 1→ 2 is greater than 2 → 1. Note that the free volume within the boundary has been exaggerated for clarity. (b) Step –like structure where close-packed planes protrude into the boundary.

Grain coarsening at high T, annealing

→ metastable equil. state

: # ↓ , size ↑

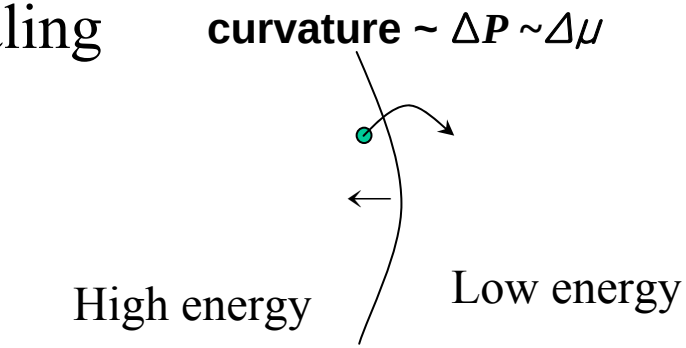

$\Delta G = 2\gamma V_m/r = \Delta\mu$

: effect of pressure difference by curved boundary

➡ Driving force for grain growth : F

V in mol : 1 (dx/V_m)

Work : F dx = ($2\gamma V_m/r$) (dx/V_m)

→ $F = 2\gamma/r = \Delta G/V_m$ (by curvature)

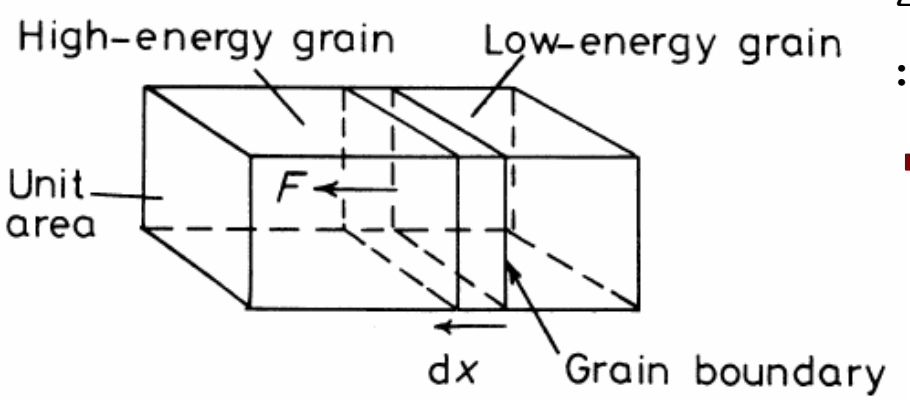

Fig. 3.25 A boundary separating grains with different free energies is subjected to a pulling force *F*.

Pulling force per unit area of boundary : $F = \dfrac{\Delta G}{V_m} \quad (N\,m^{-2})$

* How fast boundary moves ? : Grain Growth Kinetics

Grain boundary migration by thermally activated atomic jump

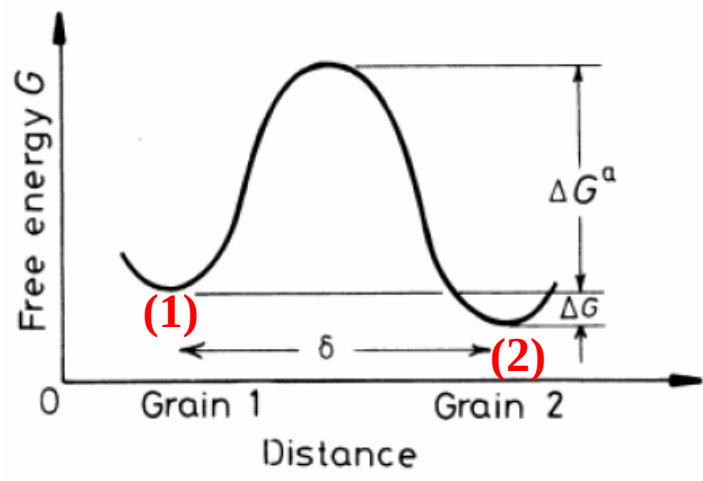

* (1) → (2) : Flux

(1) atoms in probable site : n_1

Vibration frequency : ν_1

A_2 : probability of being accommodated in grain (2)

→ $A_2 n_1 \nu_1 \exp(-\Delta G^a/RT)$ atom/m^2s = $J_{1\to2}$

* (2) →(1) flux

→ $A_1 n_2 \nu_2 \exp[-(\Delta G^a + \Delta G)/RT] = J_{2\to1}$

When $\Delta G=0$, there is no net boundary movement.

$$\mathbf{A_2 n_1 \nu_1 \approx A_1 n_2 \nu_2 = An\nu}$$

When $\Delta G > 0$, there will be a net flux from grain 1 to 2.

($A_2 n_1 \nu_1 \approx A_1 n_2 \nu_2 = An\nu$)

$$\boldsymbol{J_{1\to2} - J_{2\to1} = An\nu \exp(-\Delta G^a/RT)\,[1 - \exp(-\Delta G/RT)]}$$

- **If the boundary is moving with a velocity v, the above flux must also be equal to ?**

$$J = c \cdot v \rightarrow v/(V_m/N_a)$$

V_m/N_a : **atomic volume**

($A_2 n_1 \nu_1 \approx A_1 n_2 \nu_2 = An\nu$, if ΔG is small [$\Delta G \ll RT$])

$$J_{net} = An\nu \exp(-\Delta G^a/RT)\,[\Delta G/RT] \text{ (atom/m}^2\text{s)} = v(V_m/N_a)$$

$$v = \frac{A_2 n_1 v_1 V_m^{\,2}}{N_a RT} \exp\left(-\frac{\Delta G^a}{RT}\right)\frac{\Delta G}{V_m}$$

or $v = M \cdot \Delta G / V_m$ $\qquad$ $v \sim \Delta G/V_m$ driving force

$$\text{where } M = \left\{\frac{A_2 n_1 v_1 V_m^{\,2}}{N_a RT} \exp\left(\frac{\Delta S^a}{R}\right)\right\} \exp\left(\frac{-\Delta H^a}{RT}\right)$$

M : mobility = velocity under unit driving force ~ exp (-1/T)

The boundary migration is a thermally activated process.

Whose mobility would be high between special and random boundaries?

- High energy G.B. => Open G.B. structure => High mobility

- Low energy G.B. => closed (or dense) G.B. structure => Low mobility

Ideal ⟷ **Real**

In general,
G_b of Pure metal ⇩ on alloying

Grain Boundary Segregation

Impurities tend to stay at the GB.

$$X_b = X_0 \exp \frac{\Delta G_b}{RT}$$

X_b/X_0: GB enrichment ratio
X_0: matrix solute concentration
X_b : boundary solute concentration

ΔG_b : free energy reduced when a solute is moved to GB from matrix.

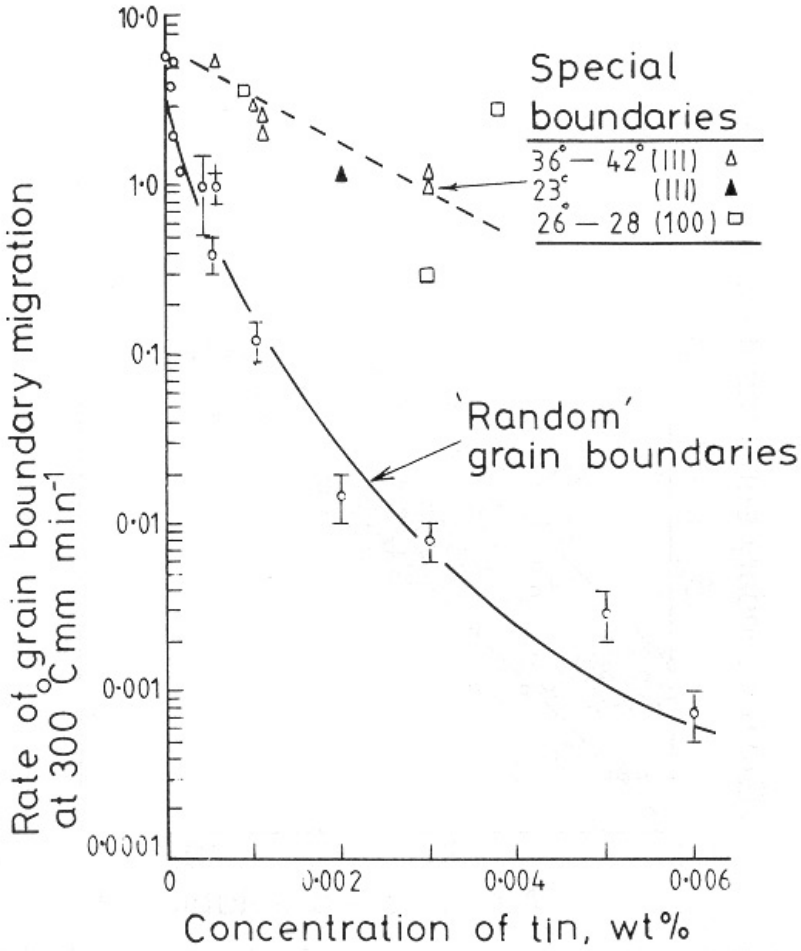

Migration rate of special and random boundaries at 300 °C in zone-refined lead alloyed with tin under equal driving forces

Schematic diagram illustrating the possible interactions of second phase particles and migrating grain boundaries.

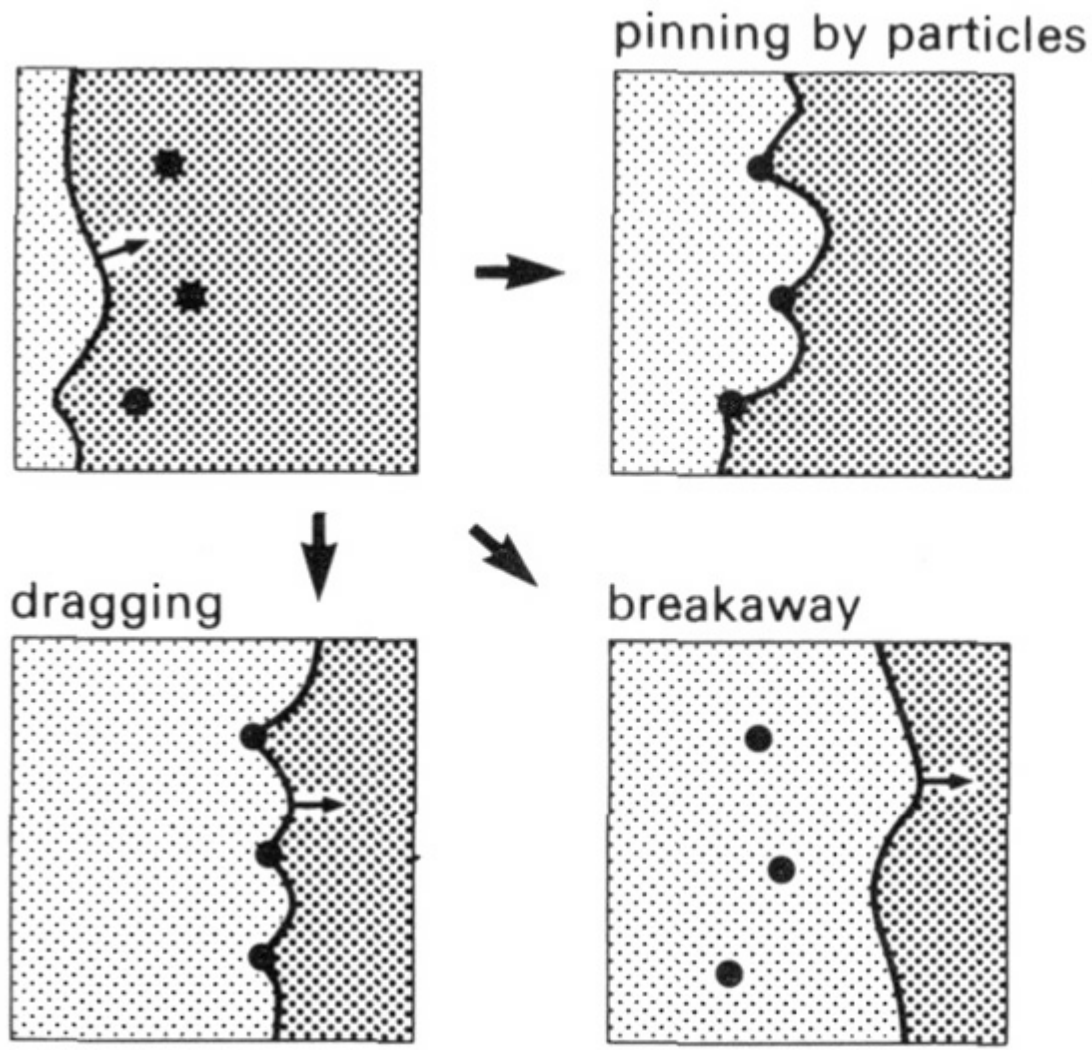

Solute drag effect

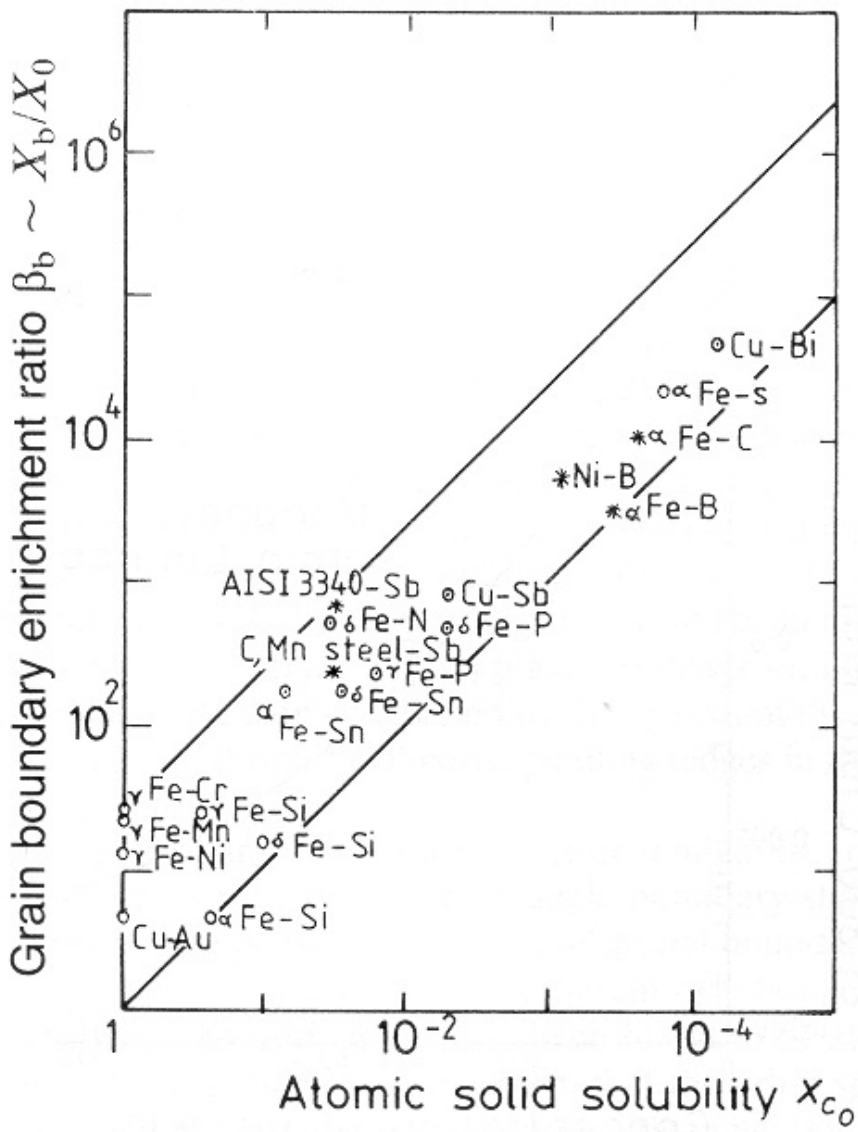

In general,
G_b and mobility of Pure metal decreases on alloying.

Generally, ΔG_b, tendency of segregation, increases as the matrix solubility decreases.

$$X_b = X_0 \exp \frac{\Delta G_b}{RT}$$

Alloying elements affects mobility of G.B.

* driving force $F = \Delta G/V_m$

$\rightarrow \quad \boldsymbol{v} = M\,(\Delta G/V_m)$

M : exponentially increase with temp.

$\boldsymbol{v}$: relation to grain coarsening

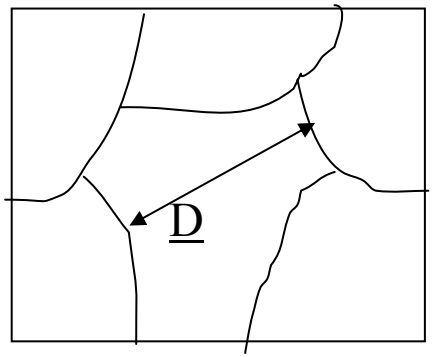

Mean grain size : $\underline{D}$

Mean radius of curvature of boundary : r

($\underline{D} \approx r$)

Mean velocity : $\underline{\boldsymbol{v}} = \alpha M\,(\Delta G/V_m) = d\underline{D}/dt$ $\qquad (\Delta G = 2\gamma V_m/r)$

$\alpha M(2\gamma/\underline{D}) = d\underline{D}/dt$ $\qquad (\alpha = \text{const} \sim 1)$

$\boldsymbol{\underline{v} \sim 1/\underline{D}\,,\ T}$

$$\rightarrow \int_{D_o}^{\underline{D}} \underline{D}\, d\underline{D} = \int 2\alpha M\gamma dt$$

$$\rightarrow \tfrac{1}{2}(\underline{D}^2 - D_o^2) = 2\alpha M\gamma t$$

$$\rightarrow (\underline{D}^2 - D_o^2) = 4\alpha M\gamma t = kt$$

$$\rightarrow \underline{D}^2 = D_o^2 + kt$$

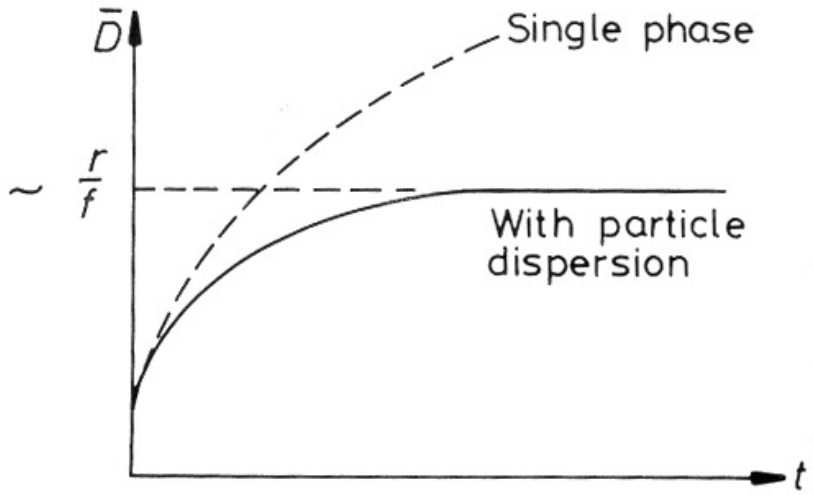

r = average radius of particles

f_v = volume fraction of particles

if $D_o \approx 0$,

$$\rightarrow \underline{D} = k't^{1/2}$$

$$\rightarrow \underline{D} = k't^n \quad \text{(experimental : } n << \tfrac{1}{2}, \tfrac{1}{2} \text{ at only high temp.)}$$

ex) (1) $D \approx 2\ \mu m \rightarrow t$?

(2) $\ln \underline{D} = \ln k' + \tfrac{1}{2} \ln t \rightarrow k'$

*** grain size : $\underline{D} = k't^n$**

→ nanostructured material D < 100nm → strength ↑

→ conventional poly-grain material D : 10~100 μm

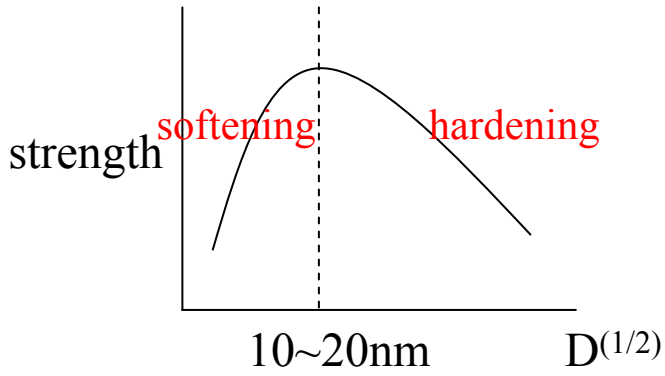

but, limited plasticity

(1) How to make nm-scale material,

→ design & processing

(2) good property : strength, corrosion resistance, wear, magnetic property

(3) bad plasticity

Normal Grain Growth

- Grain boundary moves to reduce area and total energy
- Large grain grow, small grains shrink
- Average grain size increases
- Little change of size distribution

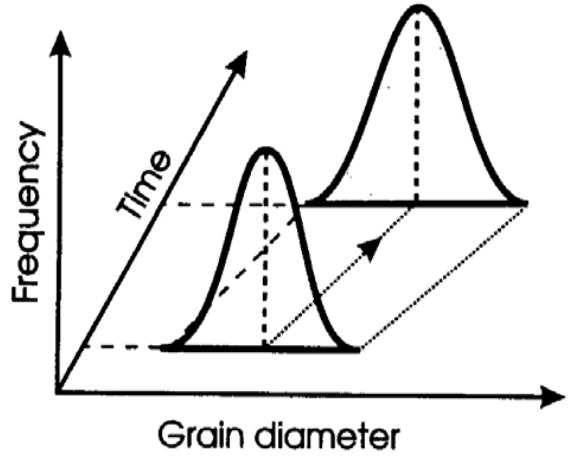

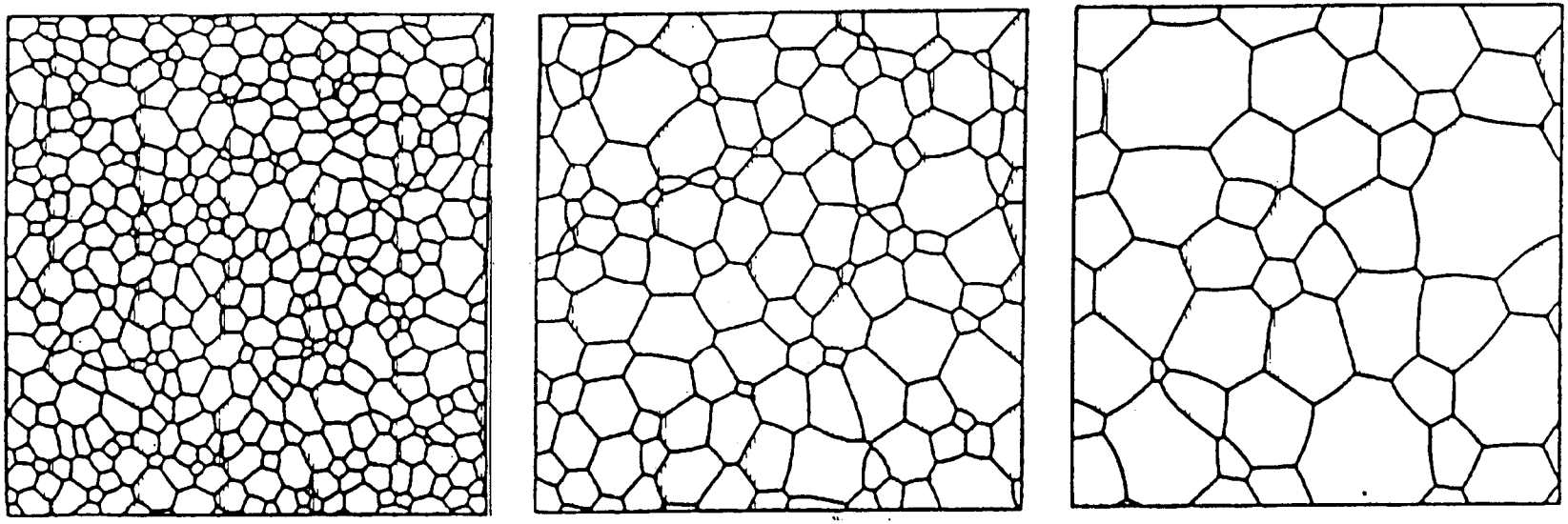

Abnormal Grain Growth

- **Discontinuous growth of a few selected grains**
  - Local breaking of pinning by precipitates
  - Anisotropy of grain boundary mobility
  - Anisotropy of surface & grain boundary energy
  - Selective segregation of impurity atoms
  - Inhomogeneity of strain energy

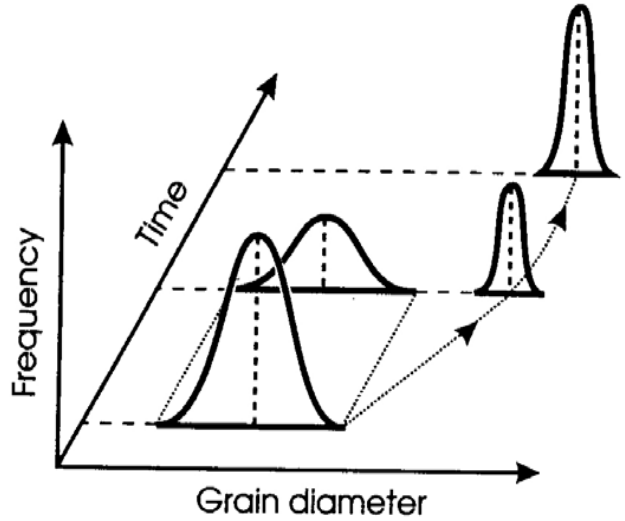

- **Bimodal Size distribution**

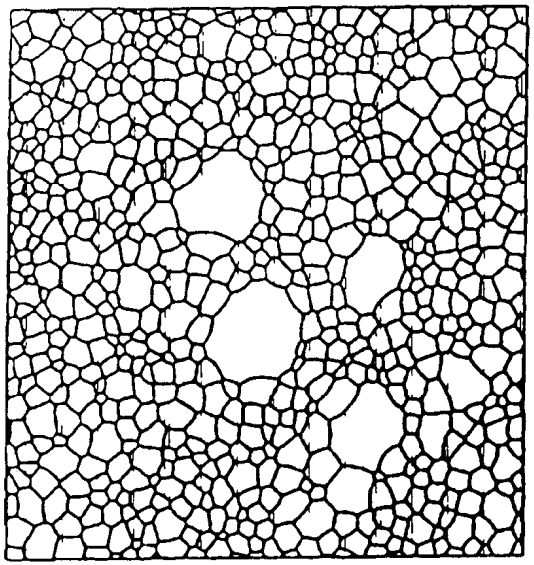

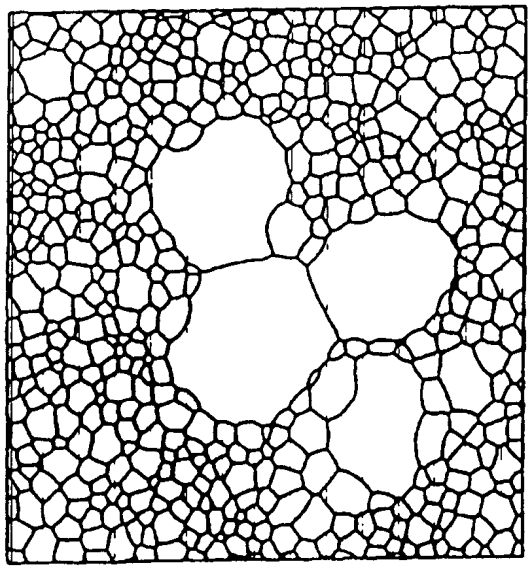

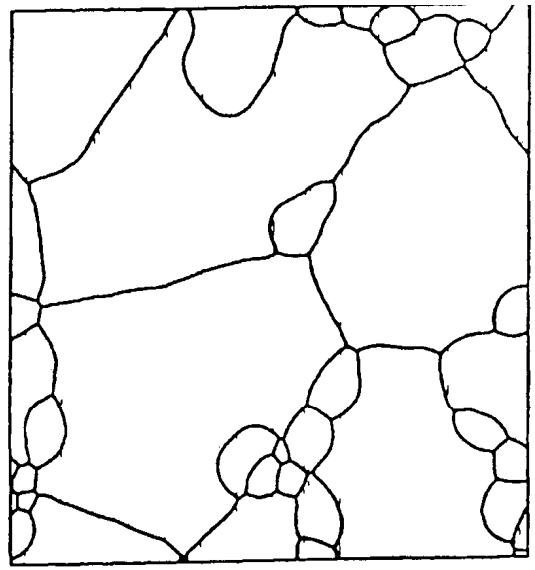

Abnormal Grain Growth
= discontinuous grain growth or secondary recrystallization

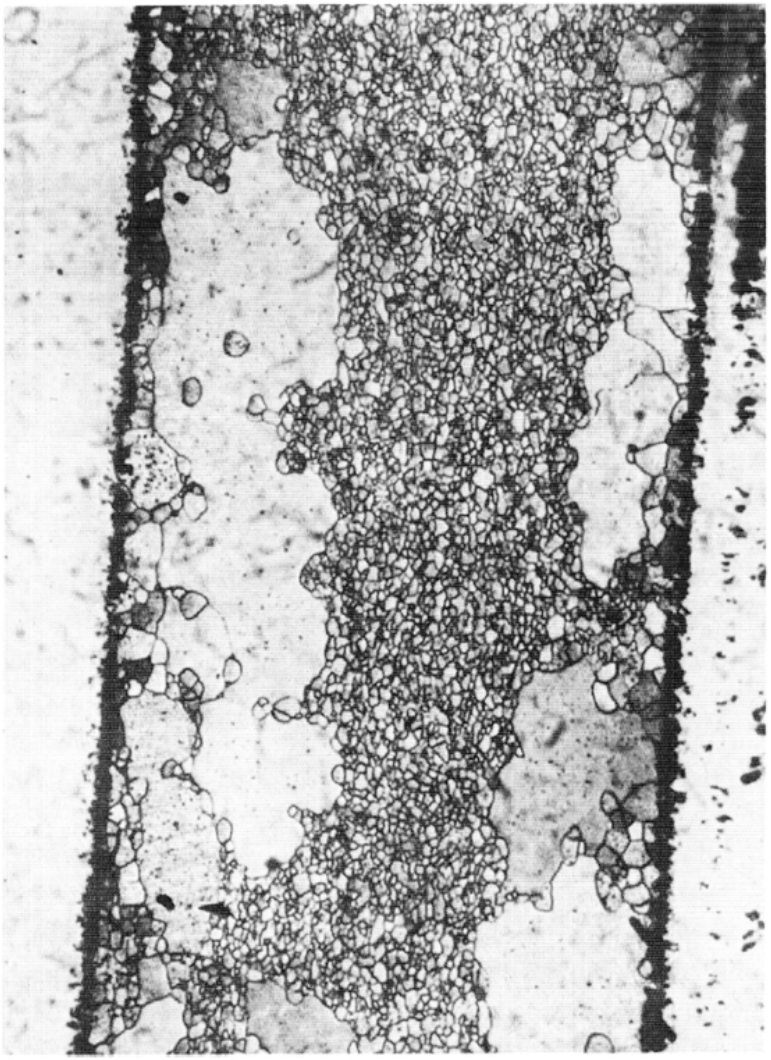

Figure 5.87 Optical micrograph showing abnormal grain growth in a fine grai steel containing 0.4 wt% carbon. The matrix grains are prevented from growing by a fine dispersion of carbide particles that are not revealed. Magnification ×135. (After Gawne and Higgins 1971. Courtesy of the Metals Society.)

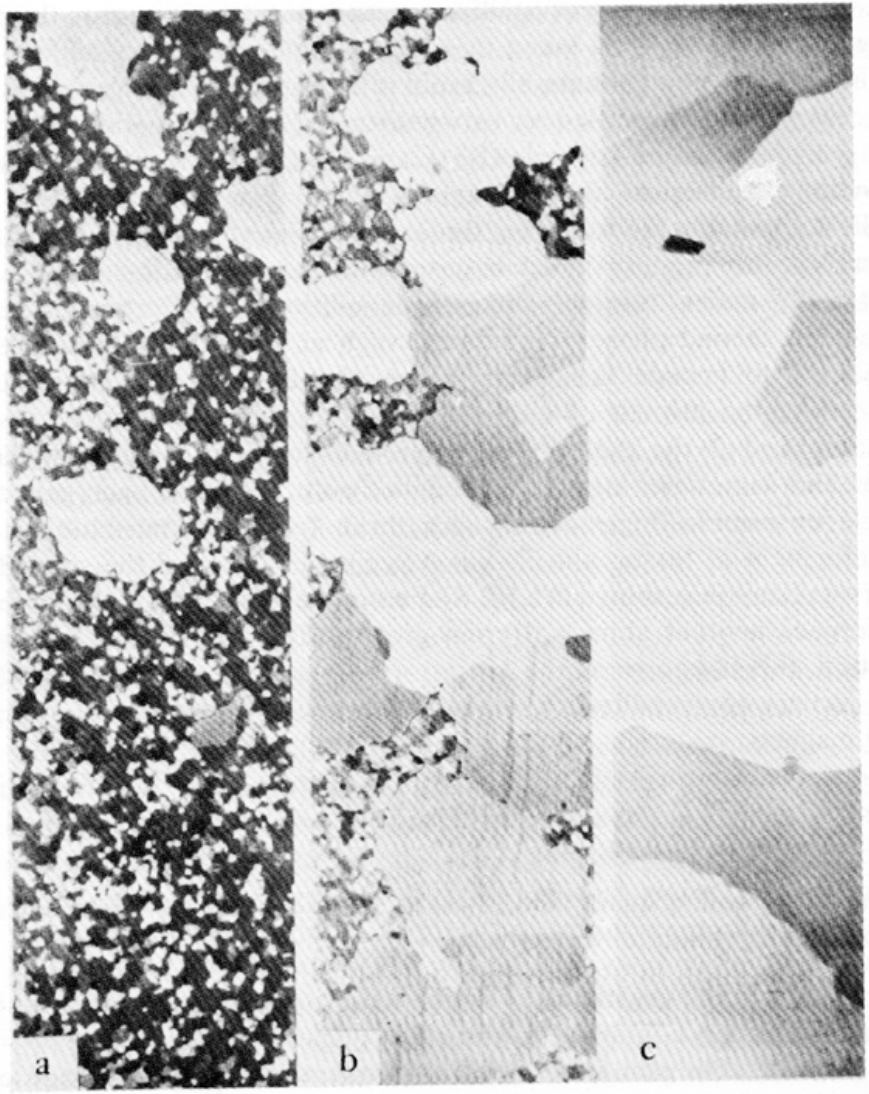

Fig. 5.48. Evidence for the preferential formation of (110)[001]-oriented grains by secondary recrystallization in 5% Si–Fe (Graham [1969]).

Pinning

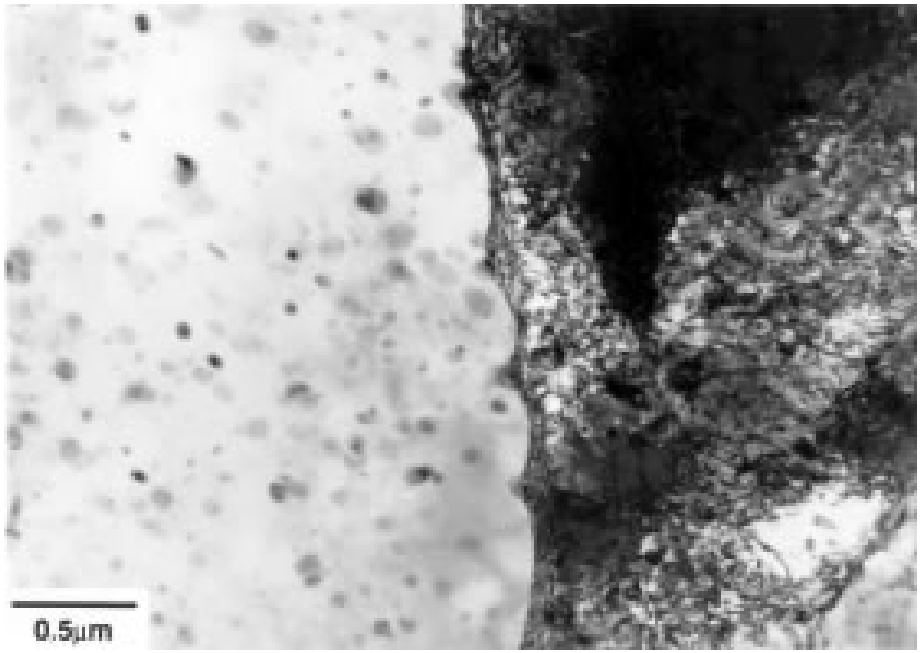

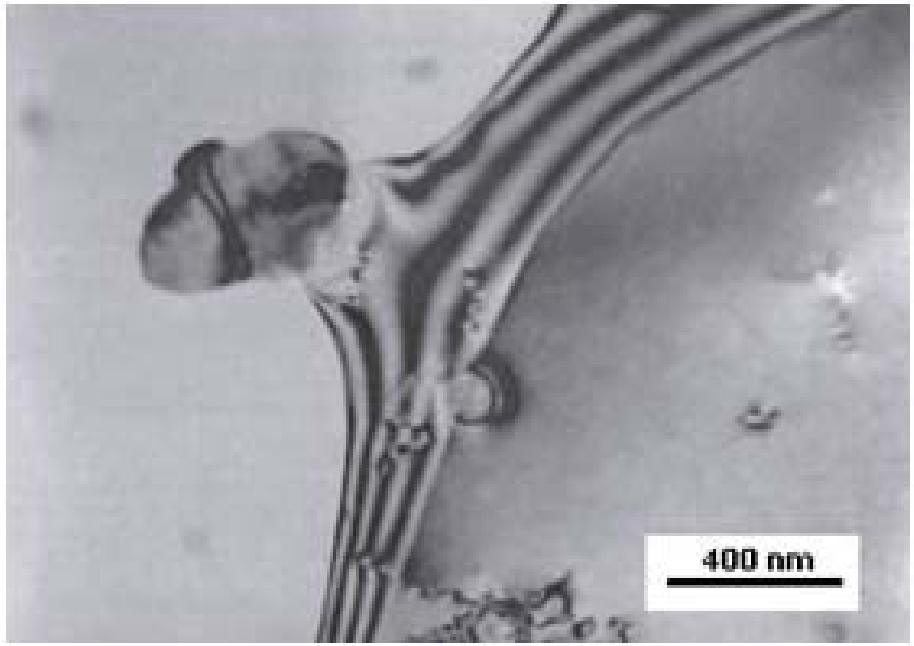

Effect of Second-Phase Particles

Interaction with particles

Zener Pinning

Derive the expression for the pinning effect of grain boundary migration by precipitates.

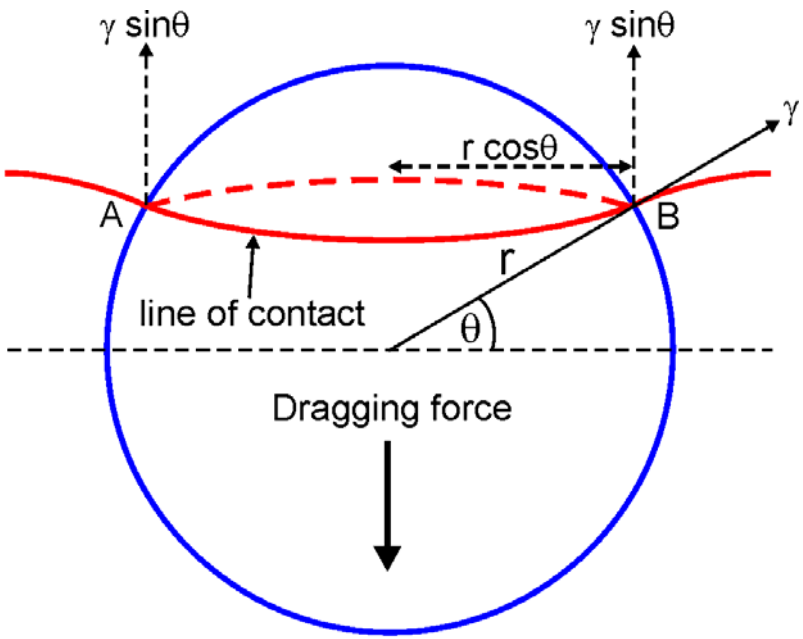

since $\gamma \sin\{\theta\} =$ force per unit length

$$F = \gamma \sin\{\theta\} \times 2\pi r \cos\{\theta\}$$ = AB

so that at $\theta = 45°$

$$F_{max} = \gamma \pi r$$

Interaction with particles

Zener Pinning

f_v = volume fraction of randomly distributed particles of radius r

N_{total} = number of particles per unit volume

$$N = \frac{f_v}{\frac{4}{3}\pi r^3}$$

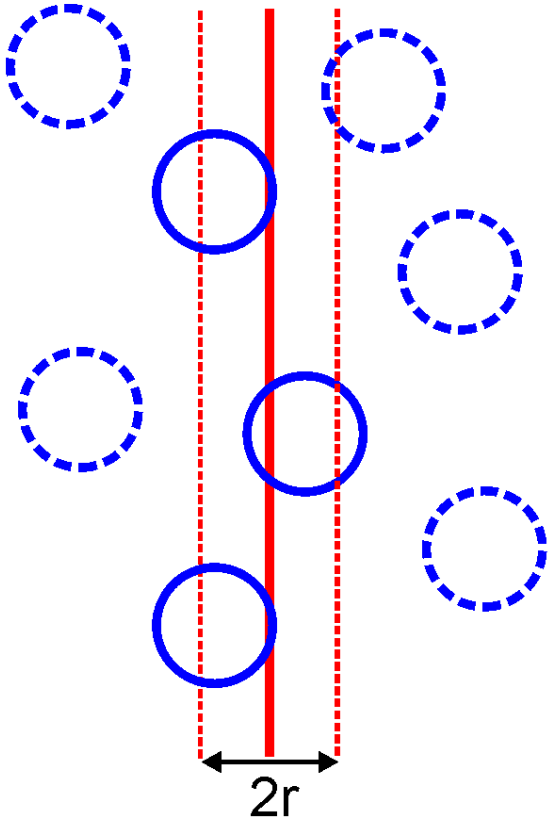

Only particles within one radius (solid circles) can intersect a planar boundary

If the boundary is essentially planar,

$$N_{interact} = 2rN_{total} = 3f_v/2\pi r^2$$

Given the assumption that all particles apply the maximum pinning force,

the total pinning pressure

$$P = \frac{3f_v}{2\pi r^2} \cdot \pi r \gamma = \frac{3f_v\gamma}{2r}$$

This force will oppose the driving force for grain growth, $2\gamma/\bar{D}$

Interaction with particles

Zener Pinning

$$P = \frac{3f_v}{2\pi r^2} \cdot \pi r \gamma = \frac{3f_v \gamma}{2r}$$

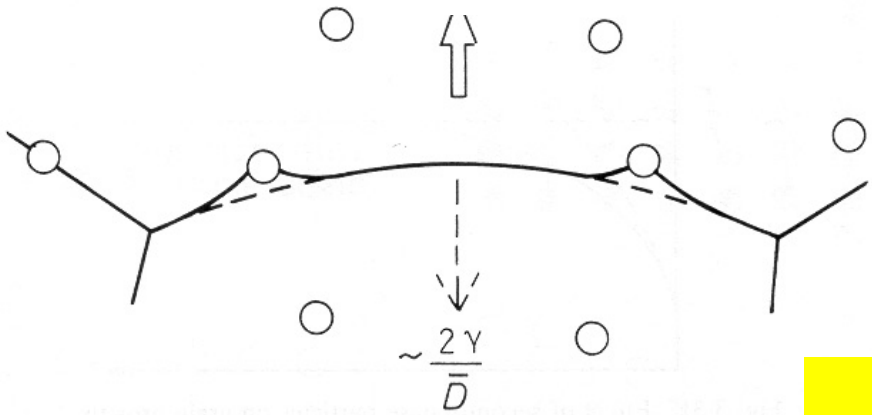

→ F = 2γ/r = ΔG/V_m (by curvature)

This force will oppose the driving force for grain growth, $2\gamma/\bar{D}$

$$\frac{2\gamma}{\bar{D}} = \frac{3f_v \gamma}{2r} \rightarrow \bar{D}_{max} = \frac{4r}{3f_v}$$

For fine grain size
→ a large volume fraction of very small particles

*** Effect of second-phase particles on grain growth**

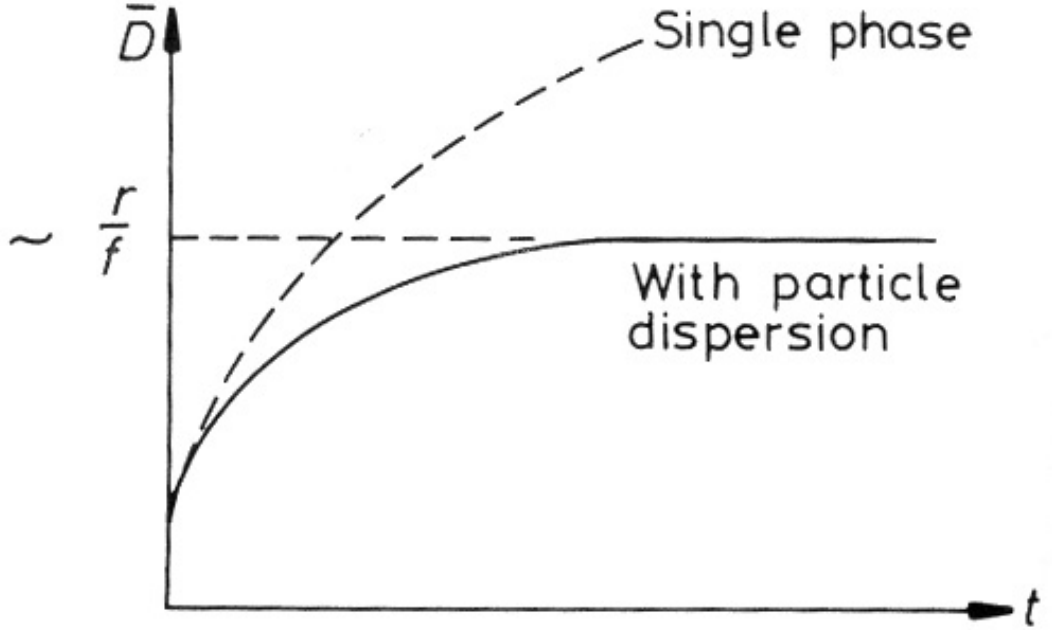

3.4 Interphase Interfaces in Solids

Interphase boundary
- different two phases : different crystal structure
different composition

Coherent,
semicoherent
incoherent

(1) Coherent interfaces Perfect atomic matching at interface

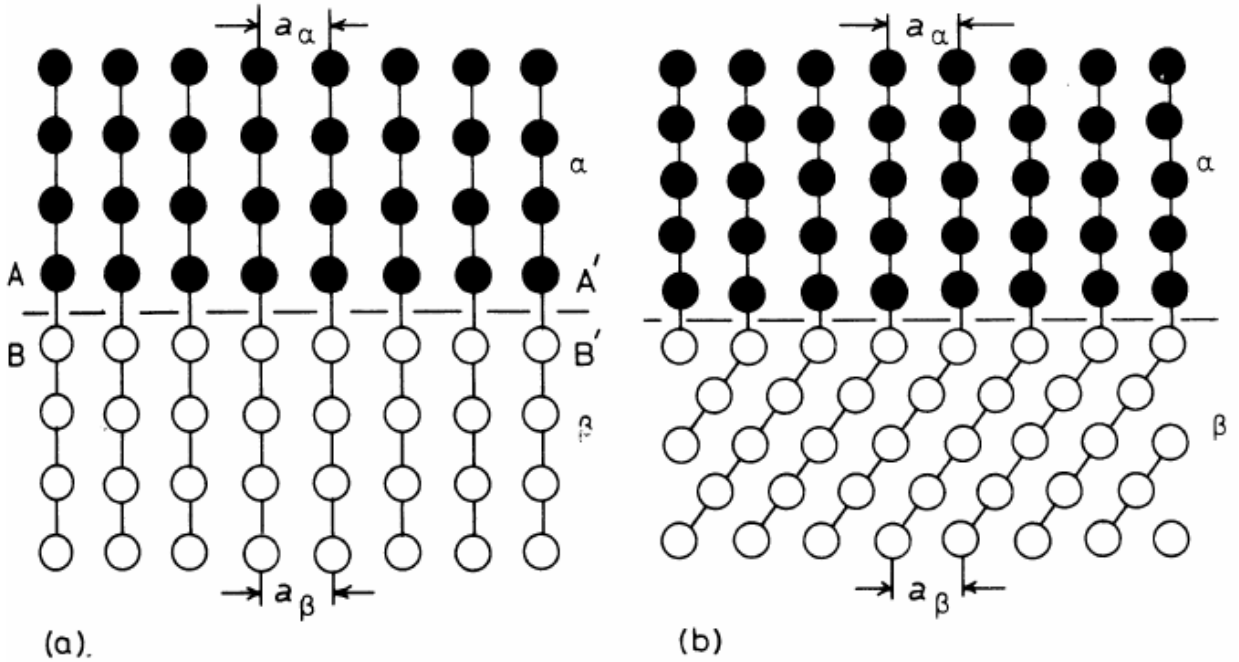

Fig. 3.32 Strain-free coherent interfaces. (a) Each crystal has a different chemical composition but the same crystal structure. (b) The two phases have different lattices.

3.4.1 Interface Coherence

Which plane and direction will be coherent between FCC and HCP?

: **Interphase interface will make lowest energy and thereby the lowest nucleation barrier**

ex) hcp silicon-rich κ phase in fcc copper-rich α matrix of Cu-Si alloy

→ the same atomic configuration

γ (coherent) = γ_{ch}

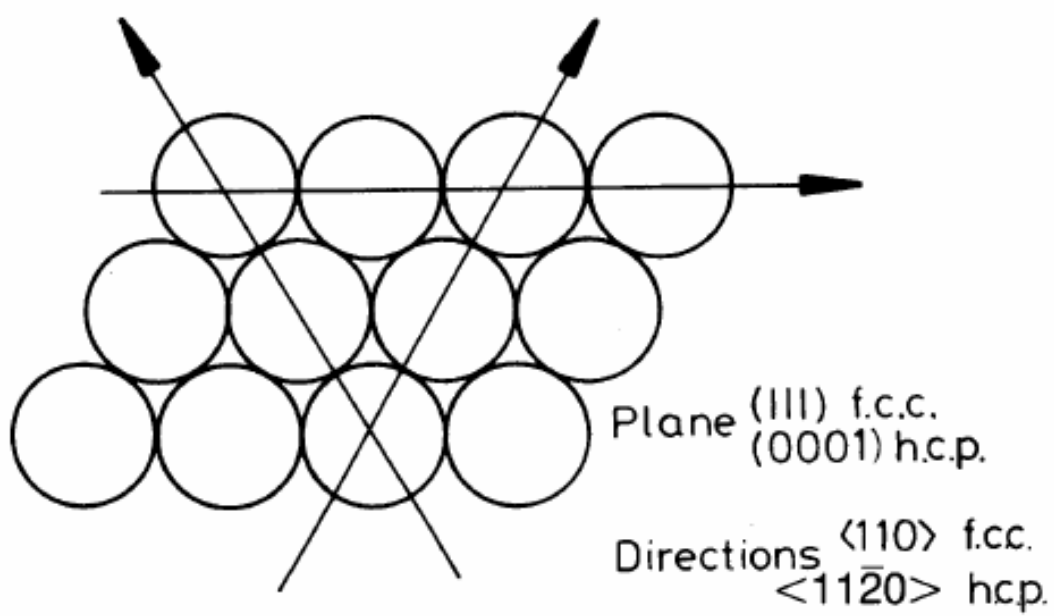

Fig. 3.33 The close-packed plane and directions in fcc and hcp structures.

→ Orientation relation

$$(111)_{\alpha} // (0001)_{\kappa}$$

$$[\bar{1}10]_{\alpha} // [11\bar{2}0]_{\kappa}$$

$\gamma_{\alpha-\kappa}$ of Cu-Si ~ 1 mJM^{-2}

In general,
γ (coherent) ~ 200 mJM^{-2}

$$\gamma_{coherent} = \gamma_{structure} + \gamma_{chemical}$$

$$= \gamma_{chemical}$$

When the atomic spacing in the interface is not identical
Between the adjacent phase, what would happen?

→ lattice distortion

→ Coherency strain

→ strain energy

Crystals are the most stable when atoms are in equilibrium spacing lie a spring.

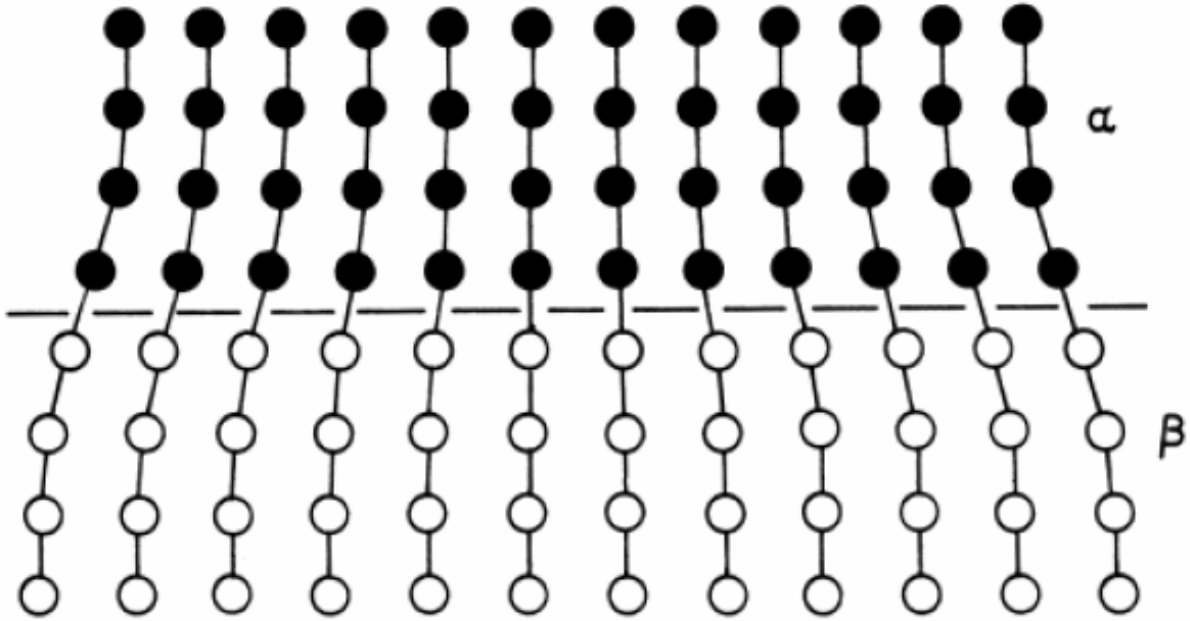

Fig. 3.34 A coherent interface with slight mismatch leads to coherency strains in the adjoining lattices.

How can this coherent strain can be reduced?

If coherency strain energy is to large, → misfit dislocations

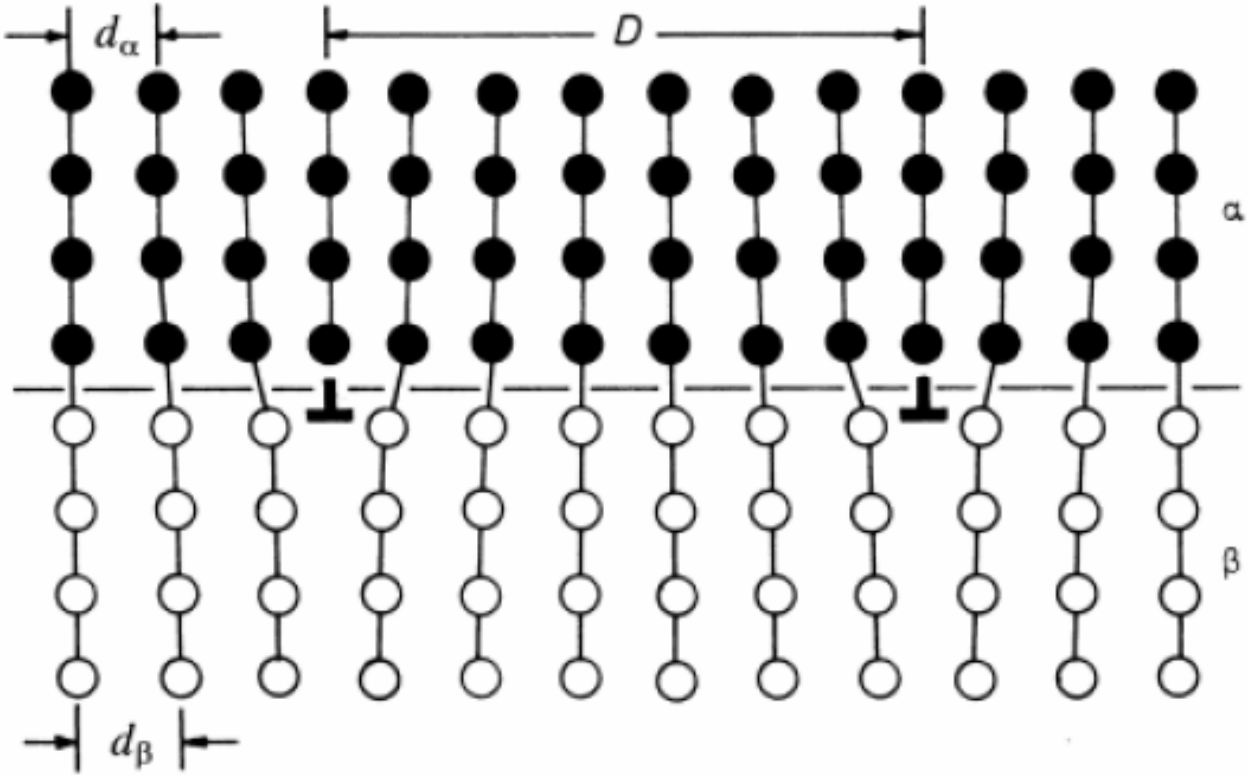

$$\delta = \frac{d_\beta - d_\alpha}{d_\alpha}$$

$$D = \frac{b}{\delta}$$

δ: misfit (disregistry)

Fig. 3.35 A semicoherent interface. The misfit parallel to the interface is accommodated by a series of edge dislocations.

(2) Semicoherent interfaces

$$\gamma(semicoherent) = \gamma_{ch} + \gamma_{st}$$

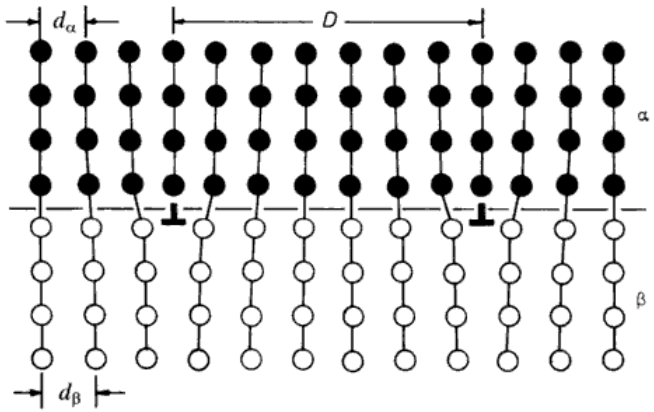

Fig. 3.35 A semicoherent interface. The misfit parallel to the interface is accommodated by a series of edge dislocations.

$d_\alpha < d_\beta$

$\gamma_{st} \propto \delta$ for small δ

γ_{st} → due to structural distortions caused by the misfit dislocations

$\gamma_{semicoherent}$: 200~500 mJ/m^2

$\delta = (d_\beta - d_\alpha)/ d_\alpha$: misfit

→ D vs. δ vs. n

$(n+1)\, d_\alpha = n\, d_\beta = D$

$\delta = (d_\beta/ d_\alpha) - 1$, $(d_\beta/ d_\alpha) = 1 + 1/n = 1 + \delta$

→ $\delta = 1/n$

$D = d_\beta / \delta \approx b / \delta$ $\quad [b=(d_\alpha + d_\beta)/2]$

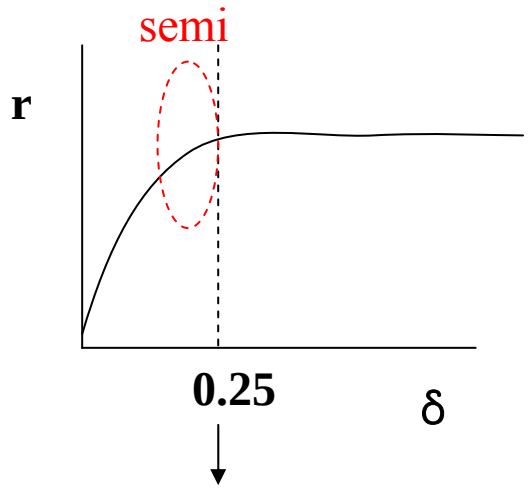

1 dislocation per 4 lattices

3) Incoherent Interfaces

$\gamma_{incoherent}$

$\rightarrow$ large $\approx 500 \sim 1000\ mJ/m^2$

1) $\delta > 0.25$

2) different crystal structure (in general)

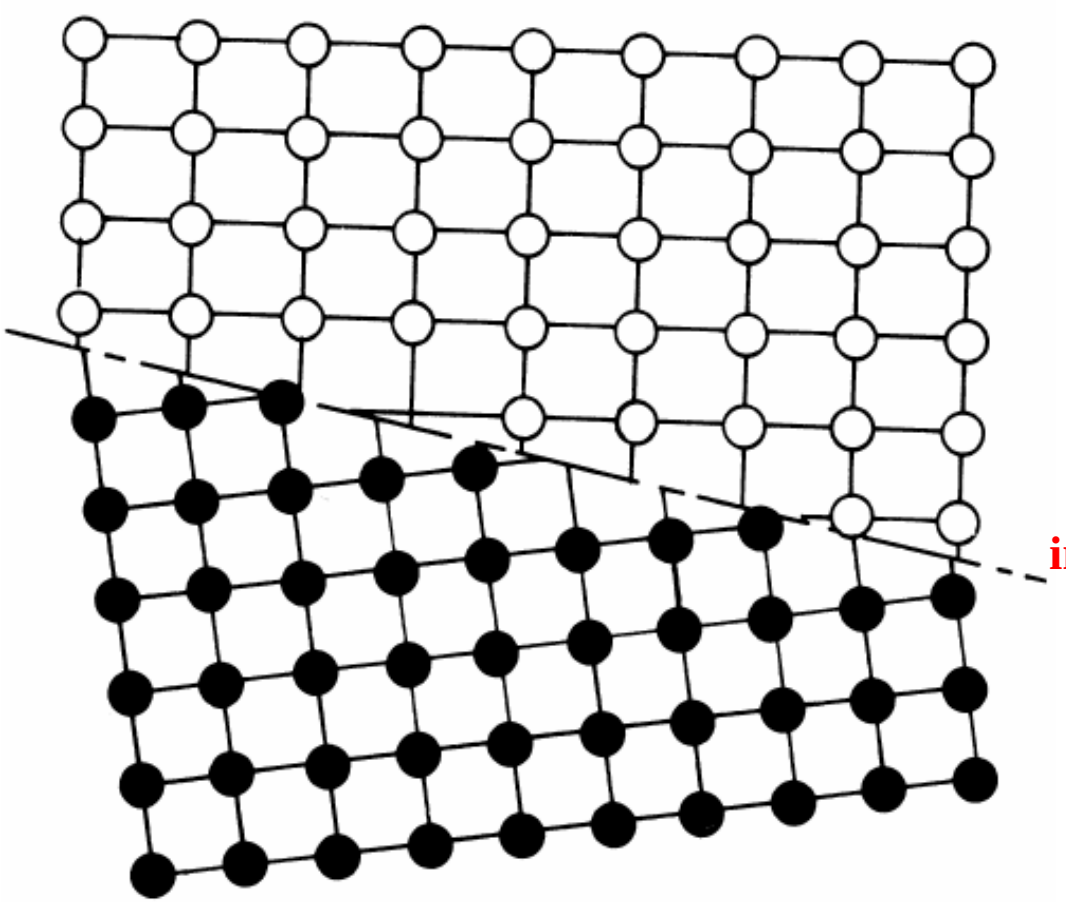

Fig. 3.37 An incoherent interface.

4) Complex Semicoherent Interfaces

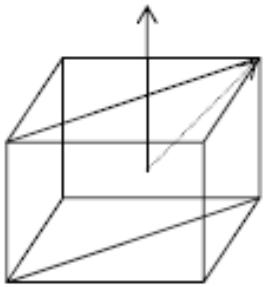

a_α=2.87

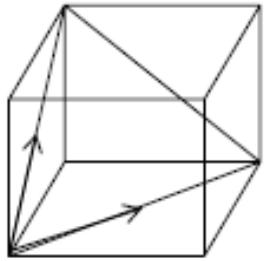

a_γ=3.57

If bcc α is precipitated from fcc γ, which interface is expected?

Which orientation would make the lowest interface energy?

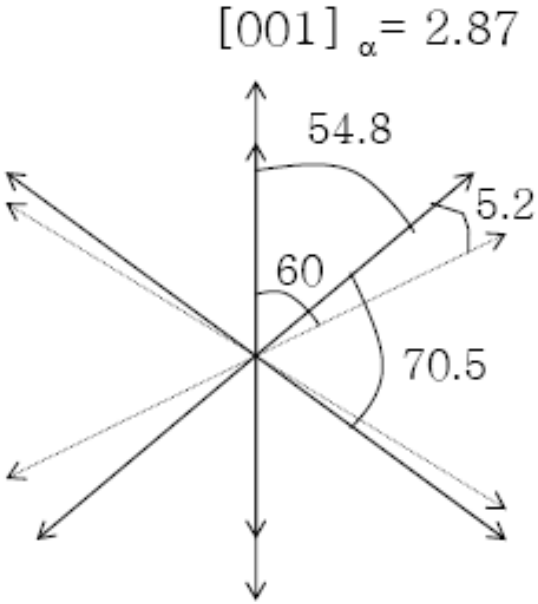

Nishiyama-Wasserman (N-W) Relationship

$$(110)_{bcc} // (111)_{fcc}, \quad [001]_{bcc} // [\bar{1}01]_{fcc}$$

Kurdjumov-Sachs (K-S) Relationships

$$(110)_{bcc} // (111)_{fcc}, \quad [1\bar{1}1]_{bcc} // [0\bar{1}1]_{fcc}$$

Complex Semicoherent Interfaces

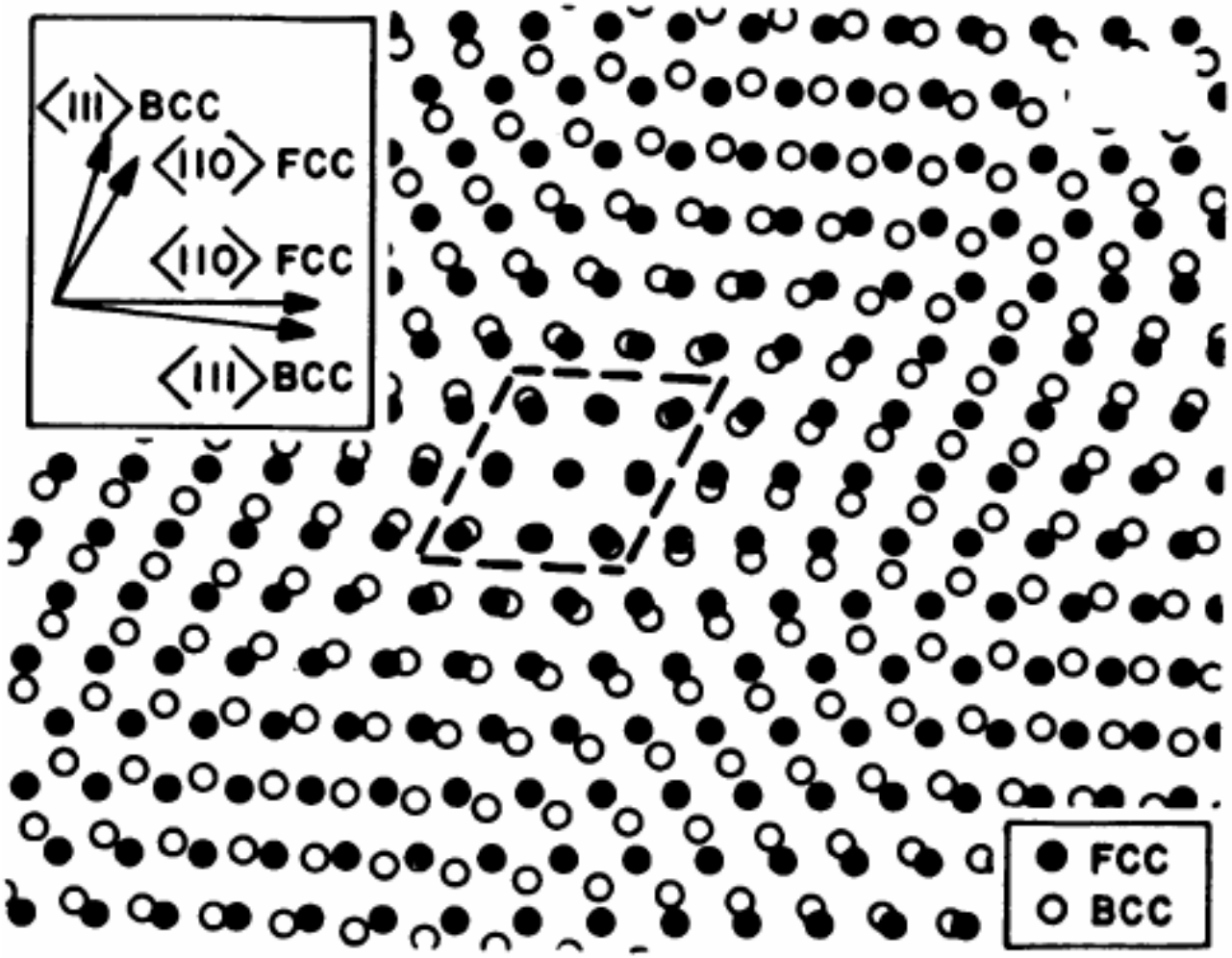

Fig. 3.38 Atomic matching across a $(111)_{fcc}/(11)_{bcc}$ interface bearing the NW orientation relationship for lattice parameters closely corresponding to the case of fcc and bcc iron. (M.G. Hall *et al.*, *Surface Science*, 31 (1972)257).